Cold Regions Science and Technology 148 (2018) 50–62

Contents lists available at ScienceDirect

Cold Regions Science and Technology

journal homepage: www.elsevier.com/locate/coldregions

3D numerical simulation of aerodynamic performance of iced contaminated wind turbine rotors

Lichun Shu, Hantao Li*, Qin Hu, Xingliang Jiang, Gang Qiu, Gaohui He, Yanqing Liu

State Key Laboratory of Power Transmission Equipment & System Security and New Technology, Chongqing University, 400044, China

ARTICLE INFO

Keywords:
Wind turbine
Computational fluid dynamics
Ice shapes
Blade aerodynamic performance
Power loss

ABSTRACT

Wind turbines often suffer from blade icing issues in cold regions, which causes the degradation of the blade aerodynamic performance and the loss of power production. In the paper, a 3D numerical simulation model of the wind turbine rotor is put forward by using a commercial computational fluid dynamics (CFD) solver ANSYS Fluent to estimate the blade aerodynamic performance after icing. The multiple reference frame (MRF) model, Reynold Averaged Navier Stokes (RANS) and *k-ω SST* turbulence model are used in the simulation. Results show that CFD computational results are in accordance with the experimental results for clean and rime-iced rotors within rated wind speed, and overrated for glaze-iced rotors at high wind speed. As the wind speed increases, the rotor speed and output power of wind turbines decrease more dramatically under icing conditions. Besides, ice shapes mainly affect pressure distribution at the leading edge of airfoils, and thus reduce the normal force and tangential force significantly at approximate 62%–89% radial position. Influenced by ice shapes, blades are more likely to work in stall region at the same wind speed. In addition, flow separation around the iced blade is more serious at larger wind speed, which will produce more momentum and frictional loss, especially for glaze ice. The results provide a valuable reference for the wind farms operation and generator system evaluation in cold regions.

1. Introduction

Wind energy is one of the most promising renewable energy sources in the future for its potential. Cold climate regions have been proved to represent an unavoidable beneficial environment for wind energy because of the higher air density and wind speed. However, wind turbines in these regions expose to icing events frequently during cold seasons, which usually bring about severe impacts: measurement errors affected by ice, complete loss or reduction of power generation, increased fatigue of components due to imbalance in the ice load, and safety hazard from ice thrown on blades (Parent and Ilinca, 2011; Battisti, 2015). With the capacity of wind turbines and the size of wind farms increasing in cold regions, the icing issues are becoming increasingly prominent, which pose a serious threat to the security and stability of wind power equipment and cause enormous economic loss to wind farms.

A large number of researches have been made on several aspects of wind turbine icing. References (Duncan et al., 2008; Homola et al., 2010a, 2010b; Virk et al., 2010) indicated that ice accretion on blades results in a reduced lift coefficient and increased drag coefficient of profiles. Fu and Farzaneh (2010) modeled the 3D rime ice accretion process on a horizontal axis wind turbine (HAWT) by using CFD approach with two phase flow. Homola et al. (2010a), (2010b) used the numerical tool to analyze the effects of temperature and droplet size variation on ice growth rate and ice shape. The results showed that streamlined ice shapes and horn shapes were observed at low and high temperature, respectively, and the characteristics were less prominent for the case of rime ice when compared to glaze ice. Lamraoui et al. (2014) investigated the impact of atmospheric icing on wind turbine production based on cylinder ice accretion model and power loss model, and found that the outer section of the blade contributed significantly to the blade aerodynamics and the power degradation can reach a maximum of 40% under icing conditions.

Several researchers performed experimental and CFD studies of aerodynamic performance degradation of wind turbines under icing conditions (Horák et al., 2008, Mortensen, 2008, Barber et al., 2010). For CFD simulations, they used a hybrid grid with structured layer near the airfoil surface and multi-block structured grids for complex glaze ice shapes to capture the boundary layer. Han et al. (2012) researched the influence of angle-of-attack, temperature, liquid water content and icing time on the ice shapes in ice accretion tests, and then analyzed icing severity effects on the wind turbine torque. Jha et al. (2012) put

* Corresponding author.
E-mail address: lht_ct@163.com (H. Li).

https://doi.org/10.1016/j.coldregions.2018.01.008
Received 21 July 2017; Received in revised form 14 November 2017; Accepted 17 January 2018

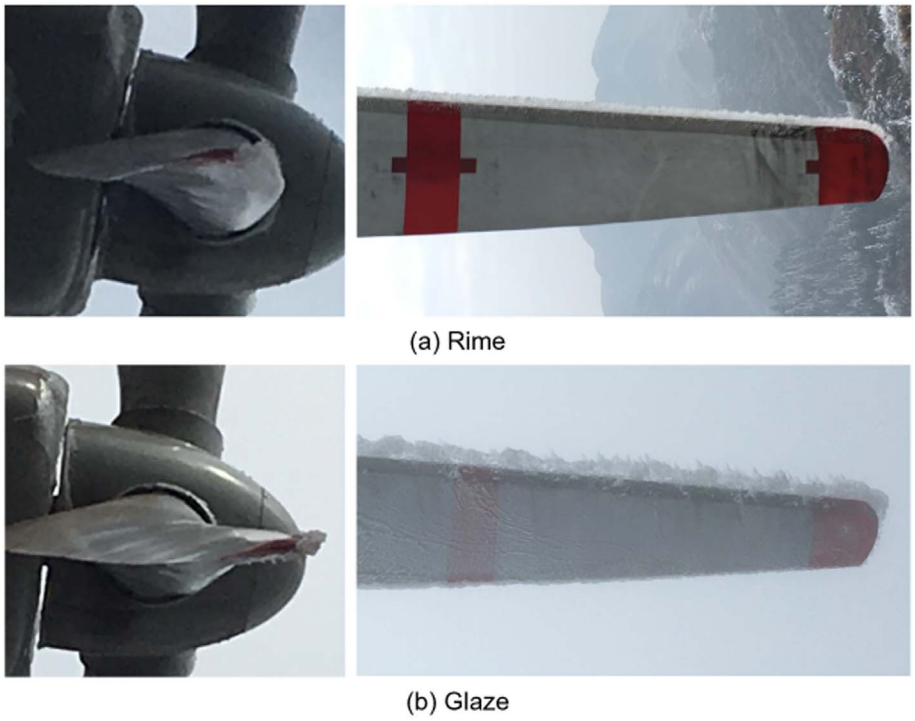

Fig. 1. Photos of 300 kW wind turbine iced blades.

Table 1
Average environmental parameters at icing events.

Icing event	RH (%)	T (°C)	V (m/s)	Time (min)
Rime	85	−11.3	6.8	120 min
Glaze	100	−1.0	12.1	180 min

forward a wind turbine icing operation control system including the ice accretion modeling, the analysis of the airfoil and wind turbine performance. In terms of 3D wind turbine flow field simulation, the CFD approaches were used to solve the Reynolds-Averaged Navier-Stokes (RANS) equations with some turbulence models, showed great agreement with experimental measurements (Duque et al., 2003; Sezeruzol and Long, 2006; Li et al., 2012; Sørensen et al., 2013).

Presently, most CFD studies on wind turbine icing only consider 2D blade profiles, which neglect 3D rotating effect with the air flow along the radial direction. Besides, the NREL Phase VI horizontal axis rotor with two blades is the usual study object in 3D CFD simulations, nevertheless, it often works with the constant rotor speed at various wind speed, which is quite different from the popular variable-pitch and variable-speed wind turbine in operation mode nowadays. In terms of the previous numerical studies on blade aerodynamics, the reduction of rotor speed caused by ice shapes is not taken into consideration. Therefore, the objective of the paper is to present a steady-state 3D CFD numerical model to investigate the impact of ice on the blade aerodynamic performance by using a commercial CFD solver ANSYS Fluent. Meanwhile, field tests under icing conditions are carried out to validate the accuracy of the model by comparing experimental and computational results. On the basis, aerodynamic mechanisms affected by ice shapes at various wind speed are analyzed comprehensively.

2. CFD numerical methods

2.1. The MRF model and governing equations

The MRF model is a steady-state approximation, in which individual cell zones can be assigned different rotational and/or translational speeds. It can provide a reasonable flow model for rotating machines in which rotor-stator interaction is relatively weak. The governing equations in each subdomain are written with respect to corresponding subdomain's reference frame. Therefore, mass and momentum equations in stationary subdomains can be written as follows:

$$\frac{\partial \rho}{\partial t} + \nabla \cdot \rho \boldsymbol{u} = 0 \tag{1}$$

$$\frac{\partial}{\partial t}(\rho \boldsymbol{u}) + \nabla \cdot (\rho \boldsymbol{u}\boldsymbol{u}) = -\nabla p + \nabla \cdot \boldsymbol{\tau} \tag{2}$$

where ρ is the air density, u is the velocity vector, p is the static pressure, τ is the stress tensor given by:

$$\boldsymbol{\tau} = v\left[(\nabla \boldsymbol{u} + \nabla \boldsymbol{u}^T) - \frac{2}{3}\nabla \cdot \boldsymbol{u} I\right] \tag{3}$$

where v is the molecular viscosity, I is the unit tensor.

Meanwhile, mass and momentum equations in moving subdomains can be written as follows:

$$\frac{\partial \rho}{\partial t} + \nabla \cdot \rho \boldsymbol{u}_r = 0 \tag{4}$$

$$\frac{\partial}{\partial t}(\rho \boldsymbol{u}_r) + \nabla \cdot (\rho \boldsymbol{u}_r \boldsymbol{u}_r) + \rho(2\boldsymbol{\omega} \times \boldsymbol{u}_r + \boldsymbol{\omega} \times \boldsymbol{\omega} \times \boldsymbol{r}) = -\nabla p + \nabla \cdot \boldsymbol{\tau}_r \tag{5}$$

where u_r is the relative velocity given by:

$$\boldsymbol{u}_r = \boldsymbol{u} - \boldsymbol{\omega} \times \boldsymbol{r} \tag{6}$$

where u is the absolute velocity, ω is the angle velocity, r is the position vector. In addition, the viscous stress $\boldsymbol{\tau}_r$ is identical to Eq. (3) except that relative velocity derivatives are used.

2.2. Turbulence model

The turbulence is modeled using a blended k-ω/k-ε shear stress transport (SST) model (Li et al., 2012), in which the turbulent kinetic energy k and specific dissipation rate ω are:

$$\frac{\partial k}{\partial t} + (\boldsymbol{u} - \sigma_k \nabla v_t) \cdot \nabla k - \frac{1}{p_k}\nabla^2 k + s_k = 0 \tag{7}$$